Coupling of Surface Plasmon Polaritons and Light in Metallic Nanoslits

K. G. Lee
Department of Physics, Seoul National University, Seoul 151-742, Korea

Q-Han Park*
Department of Physics, Korea University, Seoul, 136-701, Korea
(Received 7 February 2005; published 2 September 2005)

We clarify the nature of coupling between surface plasmon polaritons (SPP) and transmitted light in metallic nanoslit structures. The coupling strength is found to be the product of the geometric opening ratio, the aperture momentum, and the Fabry-Perot factor. We determine the effective coupling, which includes corrections due to other SPPs, and show that this effective coupling causes enhanced transmission with redshifted or blueshifted transmission peaks. Without coupling, SPP is proven to suppress transmission due to the equipartition of diffraction orders. These results show good agreement with experiment.

DOI: 10.1103/PhysRevLett.95.103902 PACS numbers: 42.70.Qs, 07.79.Fc, 42.25.−p, 73.20.Mf

The coupling of surface plasmons with light in subwavelength metallic structures has received an upsurge of interest recently as the advance of nanoscale fabrication technology makes feasible new types of photonic device tailoring light at the microscopic scale [1]. One outstanding example is the extraordinary increase of transmission through a two-dimensional array of holes in a metal film [2]. It is widely accepted that this enhanced transmission arises from the excitation of surface plasmon polaritons (SPP) in resonance with the lattice structure [3]. However, a recent numerical calculation showed that the resonant excitation of flat surface SPP, in fact, suppresses the transmission in the one-dimensional slit array [4]. Even in the hole case, experimental results indicate dips in the transmission spectrum at SPP resonances while redshifted transmission peaks appear next to dips [5]. This apparent discrepancy can be resolved by coupling SPP to other diffraction orders [6,7], also known as leaky waves [8], or by coupling SPP simply to a background radiation in analogy with the Fano resonance [9,10]. These approaches, however, either are phenomenological in that the coupling is regarded as a fitting parameter to make an agreement with experimental results or use rigorous diffraction theories that obscure the coupling by intertwining all diffraction orders. Rigorous diffraction theory also makes underlying physics implicit and becomes quickly inaccessible as the system grows more complex. In view of potential device applications utilizing complex nanoscale structures, it is highly desirable to have a causal, Feynmann-diagram-like approach to the SPP problem using building blocks. Thus the explicit characterization of coupling between SPP and light remains an important unsolved problem both academically and practically.

In this Letter, we clarify the nature of coupling between SPP and the transmitted light in metallic nanoslits. We determine the coupling strength so as to provide a quantitative description of light transmission. Specifically, we introduce the notion of "a dressed surface plasmon polariton (DSPP)," which is a simple, approximate description of a leaky wave, and show that this DSPP, indeed, forms an elementary block in the transmission problem. We show that the coupling gives rise to a shifted resonance peak of DSPP, next to a dip at SPP resonance, that is the enhanced transmission. For a well separated SPP away from other SPPs, we find the (bare) coupling constant to be the product of geometric opening ratio, the aperture momentum, and the Fabry-Perot (FP) factor. The bare coupling constant, however, changes effectively due to the presence of other SPPs. We determine the bare and the effective coupling constants and show that DSPP on the illumination side of metal film can be described sufficiently with the bare coupling, whereas DSPP on the other side requires the effective coupling obtained by including the effect of SPPs on the illumination side. Specifically, we show that the real part of the coupling constant can be either positive or negative depending on the thickness of film, and this gives rise to the redshifted or the blueshifted resonance peaks of DSPP, respectively. All these features of coupling and DSPP agree pretty well with experimental results. Finally, we prove that the resonant excitation of flat surface SPP, indeed, suppresses the transmission as well as all other SPPs corresponding to different diffraction orders. This is shown by demonstrating the "equipartition of diffraction orders," i.e., equal tangential electric field components for each SPP.

Consider a periodic array of slits, with period d and slit width a, in a metal film of thickness h deposited on a substrate as shown in Fig. 1(a). Given an incoming wave, the outgoing reflected and transmitted waves can be computed by solving Maxwell's equation and matching the relevant boundary conditions [11]. Diffraction theory assumes that the solution can be expanded in terms of diffraction orders for the reflected and the transmitted light. Using the surface impedance boundary condition for a

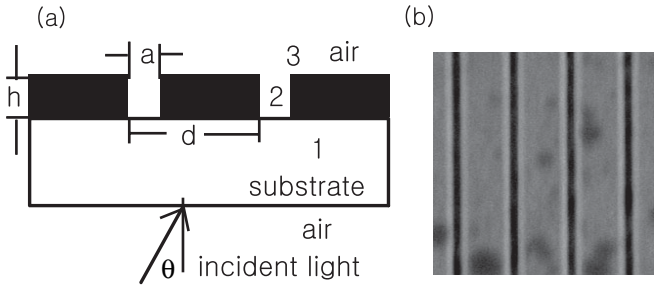

FIG. 1. (a) Schematic view of the nanoslit array on top of a substrate. (b) SEM image of slits used in experiment.

metallic surface and a single mode approximation inside slits, we subsequently determine the reflection and the transmission coefficients R_n and T_n of magnetic field parallel to the slits through the algebraic scattering equation; $\Psi_{\text{out}} = S\Psi_{\text{in}}$. That is, the outgoing wave vector $\Psi_{\text{out}} = (\{R_m\}, \{T_n\})^T$ is found from the scattering matrix S and the "slit adjusted" incoming wave vector Ψ_{in} given in a block matrix by

$$S^{-1} = \begin{pmatrix} Q^{1-} - \mu\epsilon\cot(\mu h)JK & \mu\epsilon[\sin(\mu h)]^{-1}JK \\ \mu[\sin(\mu h)]^{-1}JK & Q^{3-} - \mu\cot(\mu h)JK \end{pmatrix},$$
$$\Psi_{\text{in}} = \{\, Q_0^{1+} + \mu\epsilon\cot(\mu h)JK_0 \quad -\mu[\sin(\mu h)]^{-1}JK_0 \,\}^T. \tag{1}$$

Here, $Q_0^{1+} = \{Q_{m0}^{1+}\}$ denotes a vector and $Q^{\pm}$ is a matrix such that

$$Q_{mn}^{p\pm} = i\delta_{mn}\sqrt{\epsilon_p k_0^2 - \alpha_m^2} \pm \frac{\eta_p}{d}\int_a^d e^{-i(\alpha_m - \alpha_n)x}dx,$$
$$\alpha_m = k_0\sin\theta + \frac{2\pi m}{d}, \qquad \eta_p = -i\frac{\epsilon_p k_0}{\sqrt{\epsilon_p + \epsilon_M}}, \tag{2}$$
$$k_0 = \frac{2\pi}{\lambda},$$

where integers $m, n = -\infty, \ldots, \infty$ and $p = 1, 2, 3$ indicate three regions; the substrate, the slit, and the other side (air) with dielectric constants $\epsilon_1 = \epsilon$, $\epsilon_2 = 1$, and $\epsilon_3 = 1$. ϵ_M is the metal dielectric constant and θ is the incidence angle. JK denotes a matrix with components $J_i K_j$, and the coupling vectors J and K are defined by

$$J_m = \frac{1}{d}\int_0^a e^{-i\alpha_m x}U(x)dx, \quad K_m = \int_0^a e^{i\alpha_m x}U(x)dx. \tag{3}$$

The internal mode function $U(x)$, determined by the surface impedance boundary, is

$$U(x) = \left[\frac{\eta_2}{\beta^2} + \frac{a}{2}\left(1 + \frac{\eta_2^2}{\beta^2}\right)\right]^{-1/2}\left[\frac{\eta_2}{\beta}\sin(\beta x) + \cos(\beta x)\right], \tag{4}$$

where β is the lowest eigenvalue of the characteristic equation, $\tan(\beta a) = 2\eta_2\beta/(\beta^2 - \eta_2^2)$, and $\mu = \sqrt{k_0^2 - \beta^2}$. Since $a\eta_2 \ll 1$, $\beta \approx \sqrt{2\eta_2/a + \eta_2^2}$. Note that the scattering matrix in (1) takes the form of a matrix inverse since the outgoing reflected or transmitted waves result from an infinite sum of multiple scattering.

Having introduced a rigorous diffraction theory in a form of scattering problem, we now make a consistent simplification to treat a SPP coupled to light as an elementary block. To illustrate the nature of coupling, we focus on the spectral domain where a particular SPP, e.g., the mth order SPP in the transmission (air-metal) side, is singled out by staying away from resonance lines of other SPPs so as to neglect their contributions. This effectively reduces the scattering matrix to a 2×2 matrix,

$$S_{\text{reduced}}^{-1} = [Q^{3-} - \mu\cot(\mu h)JK]_{ij}; \qquad i, j = 0,$$
$$m \approx \begin{pmatrix} Q_{mm}^{3-} + V_b & V_b \\ V_b & Q_{00}^{3-} + V_b \end{pmatrix}, \tag{5}$$

where V_b is the bare coupling constant,

$$V_b = -\mu\cot(\mu h)\left[\int_0^a U(x)dx\right]^2 \Big/ d$$
$$\approx -(a/d)\mu\cot(\mu h). \tag{6}$$

Thus the bare coupling strength is a product of three factors—the geometrical ratio of slit opening a/d, the slit momentum μ, and the FP factor $\cot(-\mu h)$.

In the absence of coupling ($V_b = 0$), we note that SPP arises as the eigenstate of S_{reduced}^{-1} with the eigenvalue Q_{mm}^{3-} such that $T_m = 1$, $T_0 = 0$. Resonance of SPP arises when $Q_{mm}^{3-} = 0$. One can readily show that this is equivalent to the conventional expression for SPP resonance at the air-metal interface; $\lambda = \lambda_{(m)}^{\text{AM}}$,

$$\lambda_{(m)}^{AM} = \frac{2\pi d}{\sqrt{4\pi^2 m^2 - d^2\eta_3^2}} = \frac{d}{m}\sqrt{\frac{\epsilon_M}{1 + \epsilon_M}}, \tag{7}$$

where η_3 is as in (2) and we have assumed that the factor $(d - a)/d \approx 1$. This leads us to define DSPP as an eigenstate of S_{reduced}^{-1} with $V_b \neq 0$, which turns out to be a linear superposition of the mth order SPP and the zeroth order homogeneous mode describing radiation. In other words, DSPP is a simple, approximate description of a leaky wave neglecting the coupling of SPP to all other diffraction orders. Resonance of DSPP also occurs at vanishing eigenvalue, $Q_{mm}^{3-} + V_b + \mathcal{O}(V_b^2) = 0$, or equivalently at $\lambda = \lambda_{(m)}^{\text{AM-DSPP}}$ such that

$$\lambda_{(m)}^{\text{AM-DSPP}} \approx \frac{2\pi d}{\sqrt{4\pi^2 m^2 - d^2(\eta_3 - V_b)^2}}$$
$$\approx \lambda_{(m)}^{\text{AM}} + \frac{id^2 V_b}{2\pi m^2\sqrt{1 + \epsilon_M}}. \tag{8}$$

Similarly, the reduced scattering matrix for the SPP at the substrate-metal side is

$$S_{\text{reduced}}^{-1} \approx \begin{pmatrix} Q_{mm}^{1-} + \epsilon V_b & \epsilon W_b \\ W_b & Q_{00}^{3-} + V_b \end{pmatrix}, \tag{9}$$

where V_b is as given in (6) and $W_b \approx (a/d)\mu[\sin(\mu h)]^{-1}$. Once again, we define DSPP as the eigenstate of S^{-1}_{reduced} with the corresponding eigenvalue $Q^{1-}_{mm} + \epsilon V_b + \mathcal{O}(V_b^2)$. The vanishing eigenvalue again gives rise to the resonance wavelength such that

$$\lambda^{\text{SM}-\text{DSPP}}_{(m)} \approx \frac{2\pi d\sqrt{\epsilon}}{\sqrt{4\pi^2 m^2 - d^2(\eta_1 - \epsilon V_b)^2}} \approx \lambda^{\text{SM}}_{(m)} + \frac{id^2\epsilon^2 V_b}{2\pi m^2\sqrt{\epsilon + \epsilon_M}}, \tag{10}$$

where $\lambda^{\text{SM}}_{(m)} = (d/m)\sqrt{\epsilon\epsilon_M/(\epsilon + \epsilon_M)}$ agrees with the conventional resonance condition for SPP at the substrate-metal interface.

So far, we have neglected effects of other diffraction orders in characterizing DSPP. In fact, these effects are not negligible when other diffraction orders are resonantly enhanced. For instance, in defining a DSPP at the air-metal side, we could include effectively the coupling of all diffraction orders in the reflection side simply by eliminating R_n in the scattering equation. This retains the form of the 2×2 matrix S^{-1}_{reduced} in (5) except that the bare coupling V_b changes to an effective coupling

$$V_e = V_b - \frac{a\mu^2\epsilon}{d\sin^2(\mu h)}\sum_{l,m} K_l[Q^{1-} - \mu\epsilon\cot(\mu h)JK]^{-1}_{lm} J_m. \tag{11}$$

Further modification of V_{eff} could come from the coupling of diffraction orders in the transmission side, which can also be obtained by eliminating the relevant T_n in the scattering equation. Since a sizable change of V_b results only from the diffraction orders with resonance lines close to DSPP, we need to eliminate only a few diffraction orders in practice to obtain the effective coupling. We find through explicit calculation that the bare coupling is sufficient to describe DSPP at the substrate-metal side while the effective coupling in (11) is needed for DSPP at the air-metal side. Figure 2 shows both bare and effective coupling constants and the subsequent shifts of resonance wavelength that are calculated along the resonance line of SPP of order 1 at the air-metal side (AM[1]). The effective coupling V_{eff} clearly shows the impact of SM$[-1]$, the SPP of order -1 at the substrate-metal side, where resonance lines of AM[1] and SM$[-1]$ cross about 950 nm.

In order to confirm the validity of our DSPP approach, we have measured the angle dependent transmission spectrum through an array of slits in a gold film. Nanoslit arrays are fabricated by a dry etching technique after e-beam patterning on a 120 nm thick gold film grown on a flat sapphire substrate. The slit width of the sample shown in Fig. 1(b) is about 100 nm, and the period is 650 nm. Figure 3 compares the experimentally measured transmission spectra of AM[1] and SM[1] (thick lines) with theoretical curves (thin lines) obtained by using DSPP. In the AM[1] case, we have used the value of the effective coupling constant as given in Fig. 2 and measured the transmission at incidence angle $\theta = -3°$. Since the bare coupling of SM[1] is enhanced by a factor ϵ, i.e., the dielectric constant of substrate, and coupling to other diffraction orders turns out be relatively weak, we have used the bare coupling ϵV_b in computing the DSPP spectrum in Fig. 3(b) where we have taken the incidence angle $\theta = 25°$. These results show a reasonably good agreement between theory and experiment. The location of transmission dips and peaks agree remarkably well, thereby justifying predictions of our simple model using DSPP. Importantly, we note that AM[1] and SM[1] show redshifted and blueshifted peaks, respectively, which Eqs. (8) and (10) predict to be the case because the signs of the real part of coupling are positive (redshift) and negative (blueshift), respectively. This may be compared to the case of two-dimensional hole array where only redshift arises due to the evanescence of hole modes.

The effective coupling in (11) predicts strong variations in the coupling strength and the subsequent resonance wavelength shift whenever the SPP resonance line crosses other resonance lines as in Fig. 2. These features can also be found in the angle dependent transmission shown in Fig. 4. We compared the rigorous diffraction theory result obtained by solving the scattering equation in (1) with the experimentally measured spectrum using a white light source and a CCD camera. Once again, this shows a good qualitative agreement while the absolute magnitude differs partly due to the neglect of substrate thickness in the

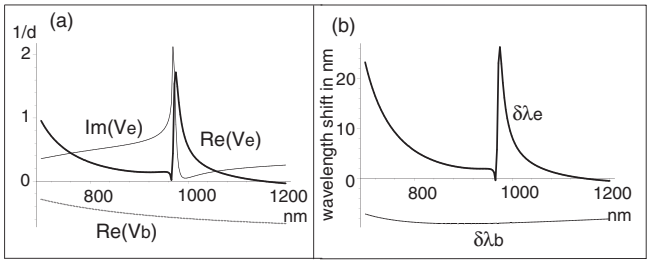

FIG. 2. (a) Bare (V_b) and effective (V_e) coupling constants calculated along the resonance line of AM[1] (air-metal side SPP of order 1). (b) Shift of resonance wavelengths of AM[1] due to bare and effective coupling.

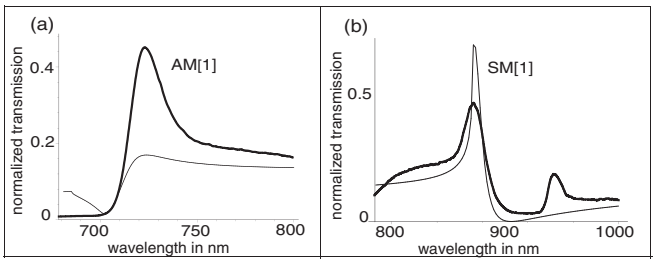

FIG. 3. Transmission spectrum of (a) SPP of order 1 at the sapphire-metal side with $\theta = -3°$ and (b) SPP of order 1 at the air-metal side with $\theta = 25°$. Thick lines are experimental results, whereas thin lines show theoretical results using DSPP.

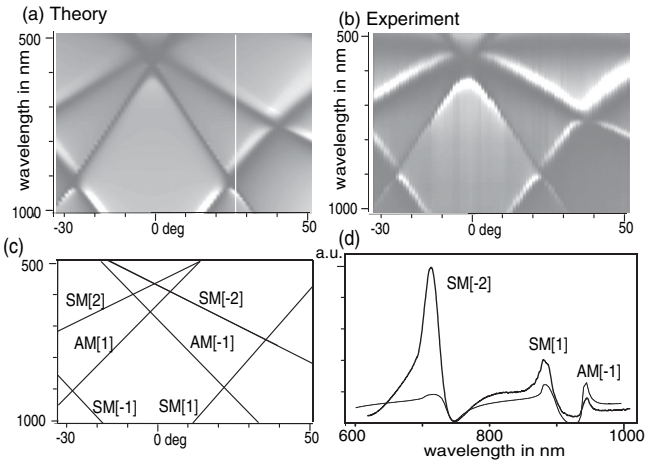

FIG. 4. Angle dependent transmission spectrum. (a) Result using rigorous diffraction theory. (b) Experimental measurement. (c) Labeling of SPP resonance lines. (d) Transmission curves at $\theta = 25°$ [crosscut in (a)] showing blueshifted and redshifted SPPs obtained by theory (thin line) and experiment (thick line).

theory calculation. Despite this, the redshifted vs the blueshifted features for AM and SM SPPs agree remarkably well. Along the resonance line of AM[1] as depicted in Fig. 4(c), both theory and experiment show the redshifted AM[1] with varying magnitudes, which are in accordance with the prediction in Fig. 2(b). The crosscut view of transmission at incidence angle $\theta = 25°$ in Fig. 4(d) demonstrates explicitly the redshifted AM$[-1]$ and the blueshifted SM$[-2]$ and SM[1] of both theory and experiment. All these features agree with predictions of our simplified DSPP approach.

Finally, we focus our attention on dips in transmission caused by SPP. We observe that the scattering equation given in (1) can be rewritten as $Q^{3-}T = \gamma J$ and $Q^{1-}R = \delta J + Q_0^{1+}$ where γ and δ are scalar functions of R and T whose detailed forms are irrelevant. Since the off-diagonal elements of Q matrix are small compared to the diagonal part by a factor a/d, we may regard Q as a diagonal matrix for narrow slits. Physically, vectors $Q^{1-}T = \{Q_{mm}^{1-}T_m\}$ and $Q^{3-}R = \{Q_{mm}^{3-}R_m\}$ represent the tangential electric field component of each diffraction order under the influence of a metal surface. Thus we find that these vectors are all proportional to the coupling vector J. Up to the leading order in a/d, components J_m are all equal so that we have equal tangential electric field components for all diffraction orders, namely, *the equipartition of diffraction orders.* An immediate consequence of the equipartition of diffraction orders is the suppression of light transmission by SPP. Recall that the resonance condition of SPP with the lattice structure is $Q_{mm}^{3-} = 0$. Since the equipartition requires that $Q_{11}^{3-}T_1 = Q_{22}^{3-}T_2 = \cdots = Q_{mm}^{3-}T_m$, vanishing Q_{mm}^{3-} with $T_m \neq 0$ implies that $T_k \approx 0$ for all $k \neq m$. Similarly, we have $R_k \approx 0$ for $k \neq 0$. In other words, a resonant excitation of SPP of order m suppresses all other diffraction orders including the zeroth order transmission. This is the reason behind the negative role of SPP in transmission.

In this Letter, we have clarified the nature of coupling between a surface plasmon polariton and transmitted light. Bare and effective coupling strengths are determined and a simple DSPP model is introduced to explain various features of transmission spectrum such as redshifted or blueshifted transmission peaks, which all agree with experiment. The appearance of the Fabry-Perot factor in the coupling of DSPP resolves conflict concerning the two different types of resonance, i.e., the surface plasmonic and the Fabry-Perot type, by combing them into a single DSPP. In view of potential applications of surface plasmonic structures in the future, the DSPP concept could play an important role as a basic building block for the metallic nanostructures.

We thank D. S. Kim, C. Lienau, and T. W. Ebbessen for their help. This work was supported in part by q-Psi at Hanyang University and Grant No. R01-2005-000-10477-0 from KOSEF. This work at SNU was suppored by MOST, KOSEF, and MOCIE.

*Corresponding author.
Electronic address: qpark@korea.ac.kr

[1] See, for example, W. Barnes, A. Dereux, and T. Ebbesen, Nature (London) **424**, 824 (2003).
[2] T. W. Ebbesen, H. J. Lezec, H. F. Ghaemi, T. Thio, and P. A. Wolff, Nature (London) **391**, 667 (1998).
[3] L. Martín-Moreno, F. J. García-Vidal, H. J. Lezec, K. M. Pellerin, T. Thio, J. B. Pendry, and T. W. Ebbesen, Phys. Rev. Lett. **86**, 1114 (2001).
[4] Q. Cao and P. Lalanne, Phys. Rev. Lett. **88**, 057403 (2002).
[5] H. F. Ghaemi, T. Thio, D. E. Grupp, T. W. Ebbesen, and H. J. Lezec, Phys. Rev. B **58**, 6779 (1998); J. R. Suckling *et al.*, Phys. Rev. Lett. **92**, 147401 (2004).
[6] J. A. Porto, F. J. García-Vidal, and J. B. Pendry, Phys. Rev. Lett. **83**, 2845 (1999).
[7] A. M. Dykhne, A. K. Sarychev, and V. M. Shalaev, Phys. Rev. B **67**, 195402 (2003); S. A. Darmanyan, M. Nevière, and A. V. Zayats, Phys. Rev. B **70**, 075103 (2004).
[8] See, for example, A. Hessel and A. A. Oliner, Appl. Opt. **4**, 1275 (1965), and earlier references therein.
[9] M. Sarrazin, J.-P. Vigneron, and J.-M. Vigoureux, Phys. Rev. B **67**, 085415 (2003).
[10] C. Genet, M. P. van Exter, and J. P. Woerdman, Opt. Commun. **225**, 331 (2003).
[11] H. Lochbihler, Phys. Rev. B **50**, 4795 (1994).